Detection and Reduction of EMC Problems in Microwave Antenna Feed Elements

Kaloyan I. Zlatkov[1], Plamen I. Dankov[2]

Abstract – **The paper considers several spread internal EMC problems, which take place in some microwave passive non-antenna devices – parasitic radiation, "high-altitude" fields, crosstalk, grounding inefficiency, etc. Near-field scanning combined with electromagnetic simulations have been used for their prediction and detection. Several design rules have been discussed to avoid these problems in the multi-layer antenna arrays up to Ka band.**

Keywords – **crosstalk, meander lines, near-field scan, parasitic radiation, RF grounding**

I. INTRODUCTION

The EMC-aware design of PCB plates becomes very important in the microwave range. As much the operation frequency of the devices and their integration density increases, a lot of high-frequency problems additionally appears together with the traditional problems of power and low-frequency signal integrity: parasitic standing waves and RF radiation from some non-antenna components, high-order mode excitation, crosstalk between adjacent transmission lines, ineffective grounding at different levels (MMIC, chip carrier and PCB plate) etc. [1].

The need to detect and reduce these problems is extremely important in the cutting-edge design and realization of multi-layer antenna arrays for application in the modern satellite two-way communication systems for mobile platforms. The multilayer antenna arrays contain a number of RF-layers with horizontally and vertically assembled active and passive components and often the mutual influence is inevitable. Depending on the distance between the layers and the density of the feed lines and the planar components, different parasitic modes and resonance excitations might exceed the acceptable level from a system-design point of view and disturb the antenna RF performance. The unwanted inherent influences are difficult to be predicted in the preliminary design process. There exist a variety of methods for minimization of these internal EMC problems as in horizontal, as well as in vertical directions. A reasonable, simple and relative inexpensive solution in the multi-layer antennas in vertical direction is in using of appropriate microwave absorbers in order to "isolate" the layers [2, 3]. Contrariwise, the parasitic influences in horizontal direction are more difficult to avoid and usually they need another solutions without using of absorbers.

[1]Kaloyan I. Zlatkov is a PhD student in Faculty of Physics, Sofia University, Bulgaria (e-mail: kaloyan_zlatkov@abv.bg). Student member IEEE.

[2]Plamen I. Dankov is Assoc. Prof. in Faculty of Physics, Sofia University, Bulgaria (e-mail: dankov@phys.uni-sofia.bg). Member IEEE

In this paper we share our experience to predict, detect and minimize some practical design problems in multilayer antenna design and realization using RF simulations and near-field measurements up to Ka band.

II. INSERTION LOSSES AND RADIATION EFFECTS IN MEANDER MICROSTRIP LINES

A. Insertion losses in meander microstrip lines

The multilayer phased antenna arrays contain a big number of radiating elements, which feed lines need some compensation of the transmitted phases and magnitudes between the different signal paths. Because the required area is usually strongly restricted in size, microstrip lines like meanders (serpentines) can be used in the feed arrangement, which contains several right-angle mitered bends. We consider this specific line as a good example for unwanted problems in the antenna feeds. The meander line itself has radiating properties and using appropriate choice of the serpentine lengths and shapes they can radiate like traveling-wave arrays without any resonators [1, 3]. Meander lines located at computer PCB's act like effective delay lines for achieving predictable phase delay for the HF signals with relatively small waveform distortion [4].

The main problems of the meander lines are the big resonance losses and the non-regular phase delay in some frequency intervals, where parasitic resonance excitations occur [3]. Fig. 1 illustrates this resonance profile of the losses
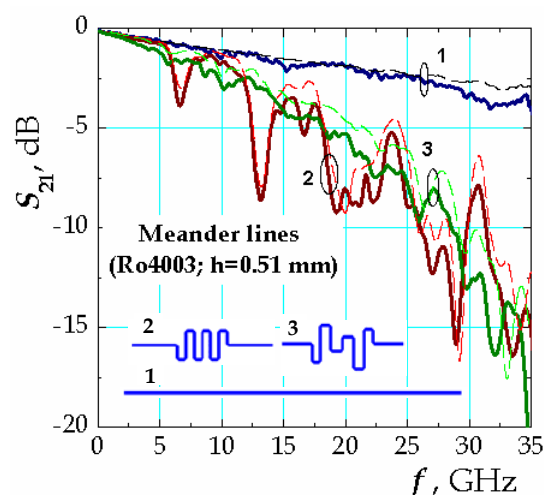
Fig. 1. Losses in antenna feed lines with equal length. Legend: 1) straight microstrip line; 2) regular meander; 3) irregular meander. Solid lines – measured losses; dashed lines – simulated loses by Zeland® IE3D

in regular meander microstrip lines, corresponding to the spurious-mode excitation. Zeland® IE3D simulator [5] is used for the analysis of regular and irregular meander microstrip lines and the simulated results are compared with the measured ones. The resonance losses appear at close-to-equidistant frequencies $f_n \sim nf_1$ ($n = 1, 2, 3…$). Maximums can be observed in the loss dependencies (at 6.8, 13.3, 20.0 GHz, etc.) that appear, when an effective Γ-junction length $\Delta_\Gamma = \Delta_X + \Delta_Y + w$ ($\Delta_\Gamma = 13.17$ mm in this case) is close to the resonance wavelength $n\lambda/2\sqrt{\varepsilon_{eff}}$ ($n = 1, 2, 3…$) of the spurious resonances (see the pictures in Fig. 2). Irregular phase delay has been observed also [3].
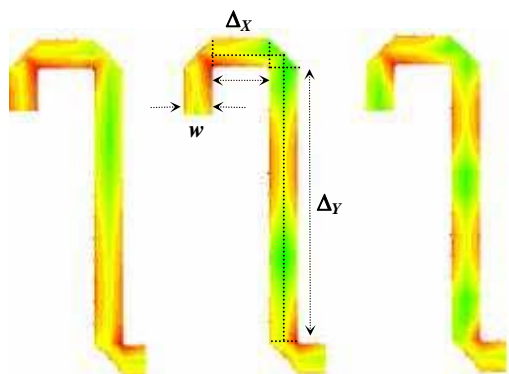
Fig 2. Simulated current distribution of the first three resonances in a single Γ-junction with effective length Δ_Γ (part of meander microstrip line); $\Delta_\Gamma = \lambda_g/2$, λ_g or $3\lambda_g/2$ (λ_g – wavelength in the microstrip line)

B. Resonance radiation in meander lines – detection by near-field scanning

The radiation effect, which appears in the regular meander line, is a very suitable phenomenon for verification of the potential of the near-field scanning (NFS) for detection of radiation effects and "high-altitude" fields over the plate surface of non-antenna devices in the microwave range [6, 7]. First, we consider a series of electromagnetic simulations performed by Zeland® IE3D [5]). The most of the 3D simulators can visualize the field magnitudes and phases on arbitrary planes, whish is very suitable to simulate a real near-
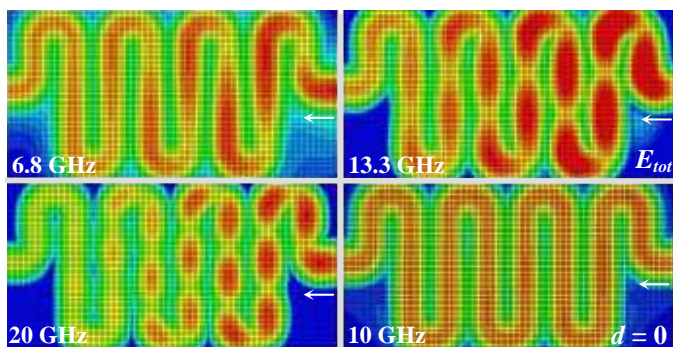
Fig. 3. Simulated near E-field distribution (by Zeland®IE3D) of the first three resonances (6.8, 13.3, 20 GHz) and for one non-resonance frequency (10 GHz) in regular meander line exactly at the substrate surface ($d = 0$). The colour scale is equal in Fig. 2-5: "red" – $1.4 \cdot 10^4$; "blue" – 100 V/m
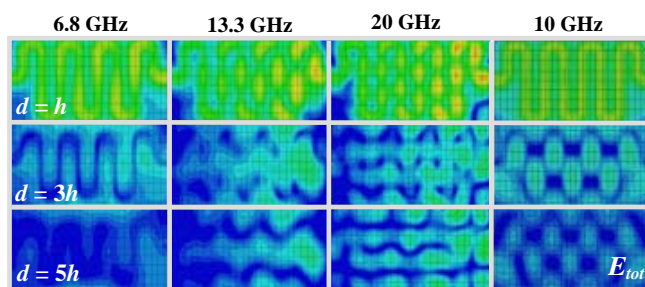
Fig. 4. Simulated near E-field distribution of the first three resonances (6.8, 13.3, 20 GHz) and for one non-resonance frequency (10 GHz) in regular meander line at different distances d from the substrate surface in horizontal slices in plane xy

field scanning [8]. Fig. 3 perfectly illustrates this ability – we can extract realistic pictures of the E-field components in horizontal xy-plane slices over the PCB substrate. The total E-field (E_{tot}) distribution exactly on the surface clearly shows the appearance of standing waves along each Γ-junction segment and the number of the resonance peaks depending on the corresponding resonance frequency. The authentic information for the field distribution is kept at the scanning distances up to $d \leq (1\text{-}1.5)h$ from the substrate surface, but at higher positions the scanned pictures lose their clearness and the standing waves are practically undistinguishable (Fig. 4). The type of the scanned field component gives also different information for the possible radiating fields. Fig. 5 shows the higher illustrative potential of the E_z component; the average potential of the E_x component, and the poor potential of the E_y component, which practically cannot detect the standing wave even at small scanning distances.

Simulated distributions of the E_z and H_z components in vertical 0z-direction (along one meander Γ-junction part Δ_Y) give additional information for the "altitude" of the radiated fields. Different simulators have been used to perform these results. The main conclusion is that the both components (E_z; H_z) are situated at very high altitudes from the plate surface
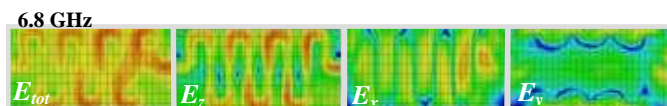
Fig. 5. Simulated near E-field components' distribution (E_x, E_y, E_z) of the first resonance (6.8 GHz) in regular meander line at distance d from the substrate surface $d = 2h$ in plane xy
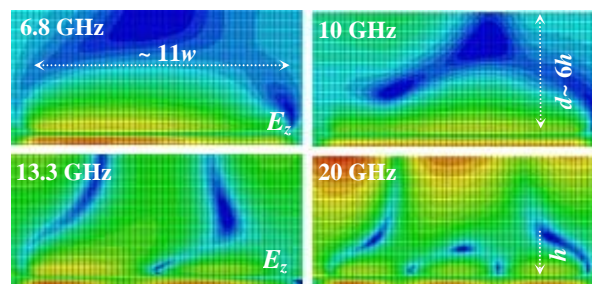
Fig. 6. Simulated near field distribution for the perpendicular component E_z of the first three resonances (6.8, 13.3, 20 GHz) and for one non-resonance frequency (10 GHz) in regular meander line in vertical plane (along one line segment Δ_Y – see Fig. 2) (simulations by Zeland®IE3D)
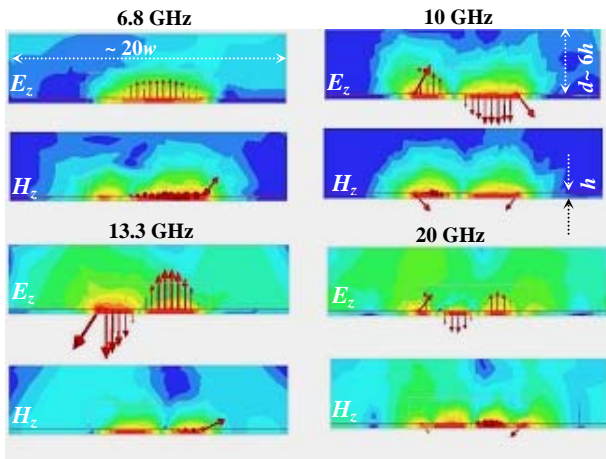
Fig. 7. Simulated near field distribution (for the perpendicular components E_z and H_z) of the first three resonances (6.8, 13.3, 20 GHz) and for one non-resonance frequency (10 GHz) in regular meander line in vertical plane along one line segment Δ_Y – see Fig. 2 (simulations by ANSYS®HFSS); color scale for H field: "red" – 50; "blue" – 0.5 A/m
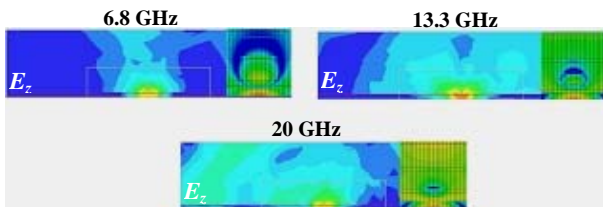
Fig. 8. Simulated near field distribution for E_z of pure microstrip line in vertical plane (the scale is like Fig. 6) (simulations by ANSYS®HFSS and Zeland®IE3D – insets on the right) (for comparison)
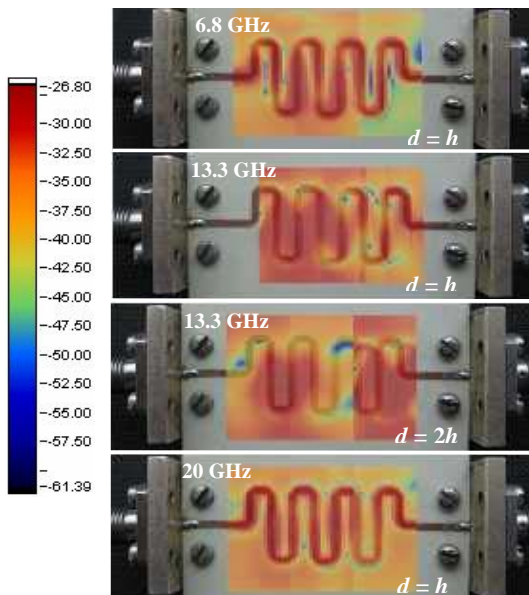
Fig. 9. Measured near E-field distribution (E_z) of the first three resonances (6.8, 13.3, 20 GHz) in regular meander line at two different distances d from the substrate surface (each picture is formed by three different scans)

for the resonance frequencies (especially at higher frequencies), compared with the vertical field distribution in regular

microstrip line (Fig. 5, 6, 7 and 8). This "high-altitude" effect is a serious problem in the regular meander feed lines in the multi-layer antenna.

Our measurements by near-field scanner over the surface of concrete meander microstrip lines (see Fig. 9) confirm the predicted field behavior at the resonance frequencies in the regular meander lines, obtained by the simulations. Informative scans can be performed at distances $d \leq h$.

C. EMC-aware design of meander lines with minimized radiation effects

How to overcome the resonance losses in the meander feed lines during the antenna design? Our investigations in [4] show that the resonance losses due to the excitation of standing waves along the serpentines can be minimized for meanders with wide horizontal section $\Delta_X > (3\text{-}4)w$. Contrariwise, when the distance Δ_X is small ($\Delta_X < 1\text{-}1.5w$), the losses at the resonances become greater due to the strong coupling between neighboring vertical sections. However, the losses far from the resonances remain smaller and close to the losses in the straight line. Similar resonance effects are observed for the phase delay. Thus, taking in mind the obtained correlation, we can optimize the meandered feeds used in planar antenna arrays in a given frequency interval. There are two possibilities for realization of feeds under preliminary given conditions (feed length and accessible area, acceptable losses and phase delay, etc.) using *regular* (Δ_Γ – fixed) or *non-regular* ($\{\Delta_\Gamma\}_j$ – varied) meander lines. The only design rule in the both cases is the length of the mitered Γ-junctions. It has to satisfy the inequality $\{\Delta_\Gamma\}_j \neq \lambda_g/2$; λ_g, $3\lambda_g/2;\ldots$ at the central frequency of the desired band (11.5-13.0 GHz in the considered example). Several optimized structures are numerically investigated to prove the applicability of this rule – see Fig. 10. The experimental data (including NFS measurements) fully confirm these results. Therefore, we can conclude, that the parameters of the optimized meandered lines are well predictable for EMC-aware design of the antenna array feeds.
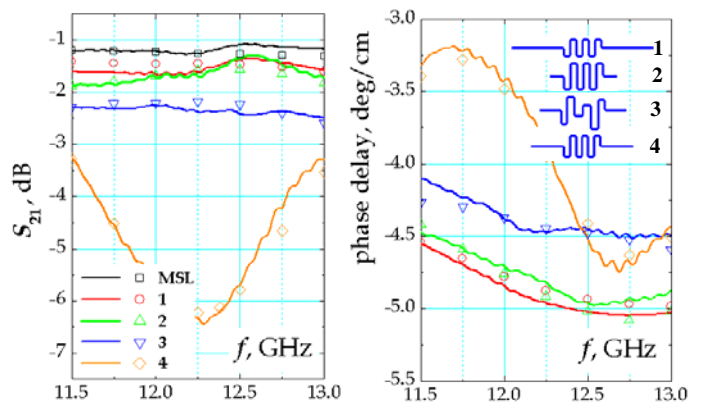
Fig. 10 [4] Calculated (solid lines) and measured (symbols) losses and phase delay in meander lines with equal length: optimal 1, 2; non-optimal 4 and irregular 3 in the frequency range 11.5-13 GHz

III "High-Altitude" Field Effect in Microwave Non-Antenna Passive Devices

The RF fields, excited far away from the PCB surface, can provoke serious problems in the active antenna feeds. Similar "high-altitude" fields exist over some open-ended, resonant, strongly coupled and high-order mode components like matching stubs, steps, T-junctions, via holes, filters, etc. The effect of these fields becomes dangerous, if the devices have to be placed in metal boxes with small height or if they have to be used in multi-layer structures with small distance between the layers.

We continue our example for the meander line losses from the previous section in order to demonstrate the importance of the "high-altitude" fields. Fig. 11 presents new results for the attenuation (dB/cm) in straight and meander lines, covered by an absorbing layer at distance Δ_A from the substrate surface [2]. The dependencies show the variations of the attenuation of the lines, when the distance Δ_A increases. The interesting circumstance here is that the influence of the absorber takes place at very high distances: Δ_A ~16-20 mm in regular meanders; Δ_A ~ 8-12 mm in irregular meanders, while only just Δ_A ~ 4 mm in the ordinary straight microstrip line. The explanation is that the RF fields over the meander line are higher than in the case of straight line and therefore the covering absorber has stronger influence on them. This behavior is fully confirmed by numerical simulations with HFSS [2]. We discuss below other examples for this EMC problem.
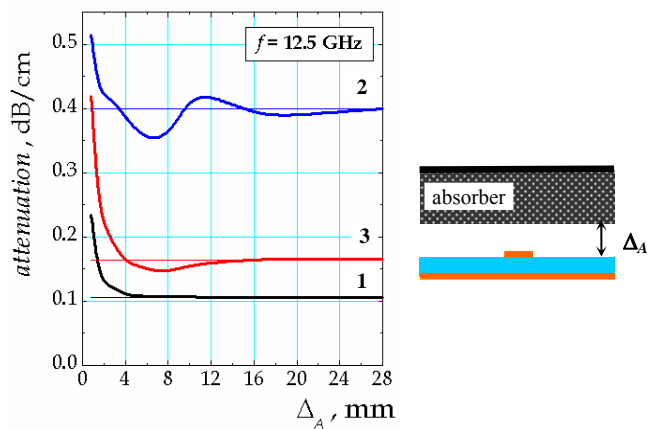
Fig. 11 [2] Measured attenuation in straight MSL line (1); regular (2) and irregular (3) meander caused by a shielded absorber layer (Eccosorb LS26), placed at distance Δ_A above the substrate

A. Near-field effects in filters and diplexers

The microwave filters in their band-stop frequency range reflect strong signals back to the RF inputs and this provokes excitation of strong standing waves with "high-altitude" fields over the mictrostrip conductor near the input. This spurious effect may easy excite the close active devices, placed in horizontal directions (e.g. amplifiers) and destroy their performances. In order to overcome this problem, an appropriate filter-diplexer can replace the problematic band-
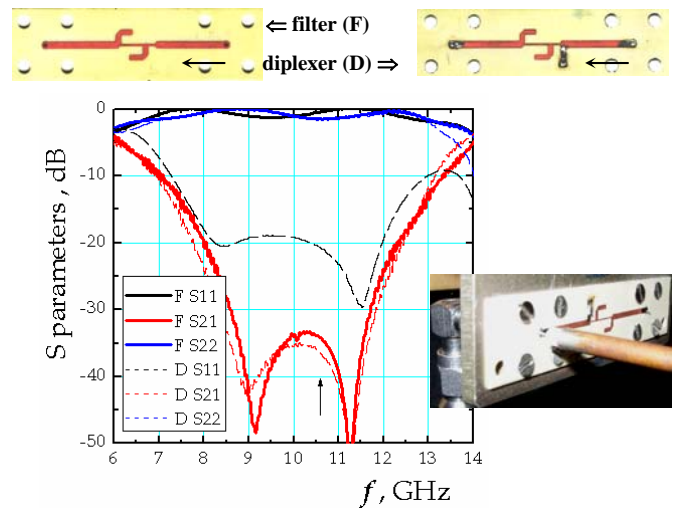
Fig. 12. Comparison between the S-parameter of filter (F) and diplexer (D), both having band-stop range 8.6-11.8 GHz
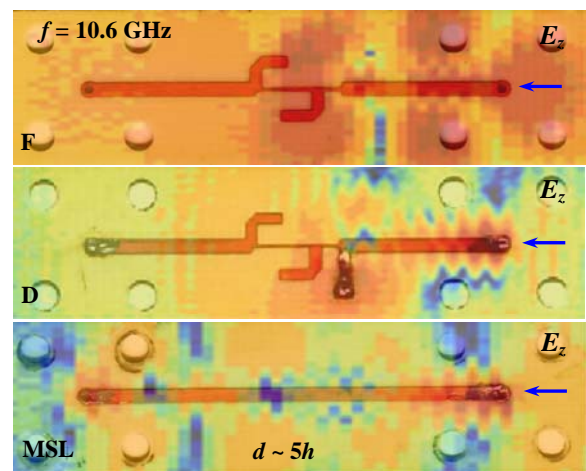
Fig. 13. Measured near-field distribution of the normal E field E_z over the substrates (RO4003; h = 0.51 mm) with band-stop filter F, diplexer D and ordinary microstrip line MSL
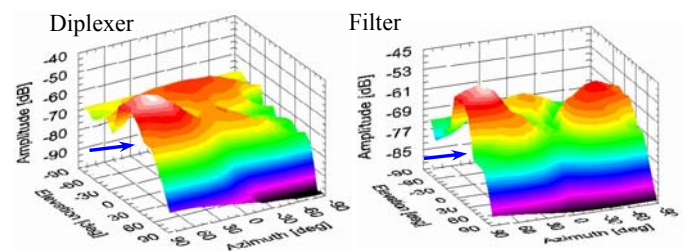
Fig. 14. 3D visualization of the near-field (E_z) magnitudes for the both devices F and D (from the 2D plots in Fig. 13)

stop filter. The filter-diplexer is considerably better matched in the band-stop range (due to the inserted 50-Ohms resistor at the input) and this property can minimize the appearance of standing waves – Fig. 12. In order to verify this assumption we have implemented NFS of these structures (Fig. 13 and 14) for the scanned E_z component at high distance d from the surface (d ~ 5h). The presented measured NFS 2D pictures are very informative for the presence of a near-field radiation near the filter inputs.

In fact, the region of stronger standing waves in the filter

and the diplexer is near to the input. The standing-wave region in the filter occupies a relatively wide region outside the input microstrip line. Contrariwise, the standing waves in the diplexer are not so widely spread outside to the input, and relatively strong high-altitude fields appear near to the 50-Ohms resistor and the grounding via holes at its end. The conclusion is that the radiating fields in the filter configurations cannot be minimized only by redistribution of the traveling waves in the band-stop range. The use of the diplexer instead of a pure filter considerably increases the matching degree with the signal source in the band-stop range. Nevertheless, the radiating fields over these structures remain strong (only a change of their polarization and direction of radiation is observed). Thus, combining this field redistribution with the classical absorption of the parasitic fringing fields by ordinary absorber layers of bulk absorbing materials, placed on the walls of the metal box, considerable minimize the considered EMC problem.

B. Near-field in hybrids and power combining devices

The power distributing devices (T-junctions, Wilkinson dividers, hybrids, etc.) play important role in the antenna feed lines. Unfortunately, they support high-order modes in the coupling region and therefore they often are sources of parasitic high-altitude fields. A simple example is the changing of the power-dividing ratio in the ordinary T-junctions after the covering of the plates with a metal screen – see Fig. 15 [2]. The simplest solution of this problem is the "isolating" of the covering screen with an appropriate sheet absorber, which compensates the screen influence, but may increase the total attenuation in the feed lines.
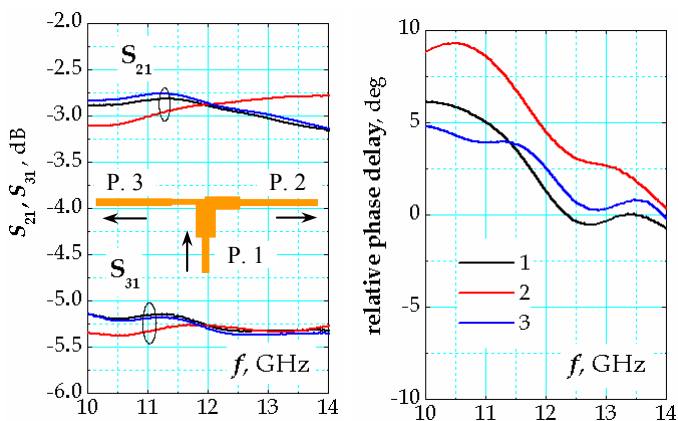
Fig. 15. Power distribution in T-junction (2:1) covered by 0.8-mm thick grounded absorber (Emmerson &Cumming BSR-1); Legend: 1) pure T-junction; 2) T-junction covered by metal screen at 5 mm; 3) T-junction covered by absorber and metal screen at 5 mm.

Another popular device for power distribution in the antenna feed lines is the quadrature hybrid (Fig. 16). This device has quarter-wavelength resonance parts in its structure and supports stable field/current distribution over its surface along the series and parallel sections, illustrated by the NFS distribution of the magnetic $H_{x,y}$ components in Fig. 17, 18. Usually, the fields over the hybrid sections at low frequency
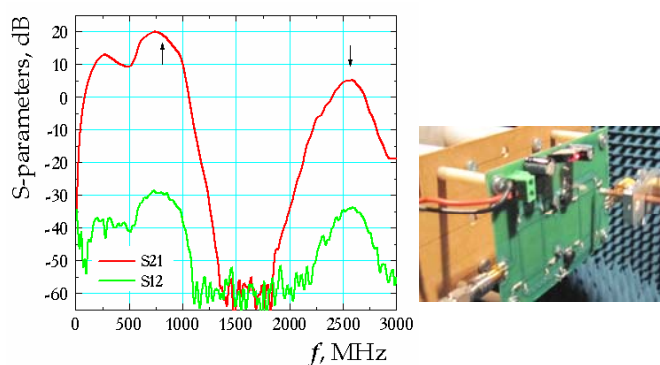
Fig. 16. Measured gain of balanced power amplifier for GSM bands containing 2 hybrids at the input and at the output. The device has 2 frequency bandwidths, marked with arrows – operational (~812 MHz) and parasitic (~2520 MHz)
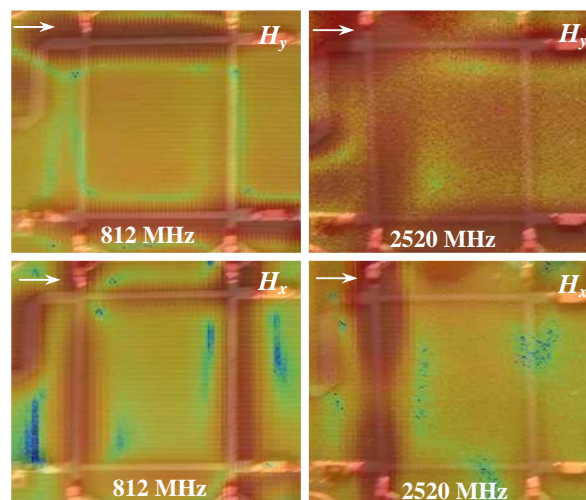
Fig. 17. Measured $H_{x,y}$ components by NFS over the input hybrids from Fig. 16. Two different modes can be detected.
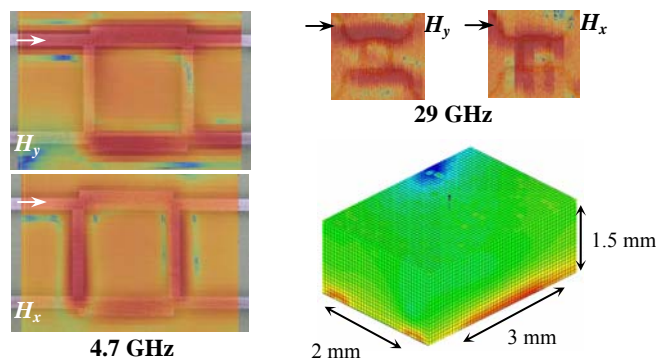
Fig. 18. Measured $H_{x,y}$ components by NFS over hybrids for C and Ka band (the fields can be detected even at $12h$ and more)

are situated close to the surface compared with h and they are not dangerous, but at higher frequencies the fields' altitude increases and putting the hybrid in a metal box becomes problematic. The hybrids can support also high-order modes, which leads to the existence of parasitic frequency bandwidths (see Fig. 16). The NFS of the 3rd-order mode fields in the hybrid clearly shows its excitation and the relatively strong field magnitudes, compared to the 1st-order mode fields (Fig. 17).

IV. CROSSTALK IN THE PLANAR TRANSMISSION-LINE FEEDS

The crosstalk (RF-signal penetration from one transmission line to other in the case of big proximity) is a "classical" internal EMC problem in horizontal direction, especially at high frequencies. The problem becomes very important in the antenna feeds, because the crosstalk causes changes in the signal magnitude in the coupled line, as well as in the phase delay in the main line [9]. The results from a short numerical investigation (by Zeland®IE3D) of three coupled lines: pair of microstrips, pair of shielded microstrips and pair of grounded coplanar waveguides are shown in Fig. 19. The horizontal shielding in a pair of coupling microstrip lines decreases the crosstalk magnitudes, but utilization of grounded coplanar waveguides is more efficient. Unfortunately, a dense array of grounding via holes has to be used in this case in order to keep the ground potential in the intermediate tape and to prevent the parasitic crosstalk. The optimal distance between the via holes is equal to quarter wavelength or slightly less, and the via-holes edges should be close as much as possible to the ground tape edge.
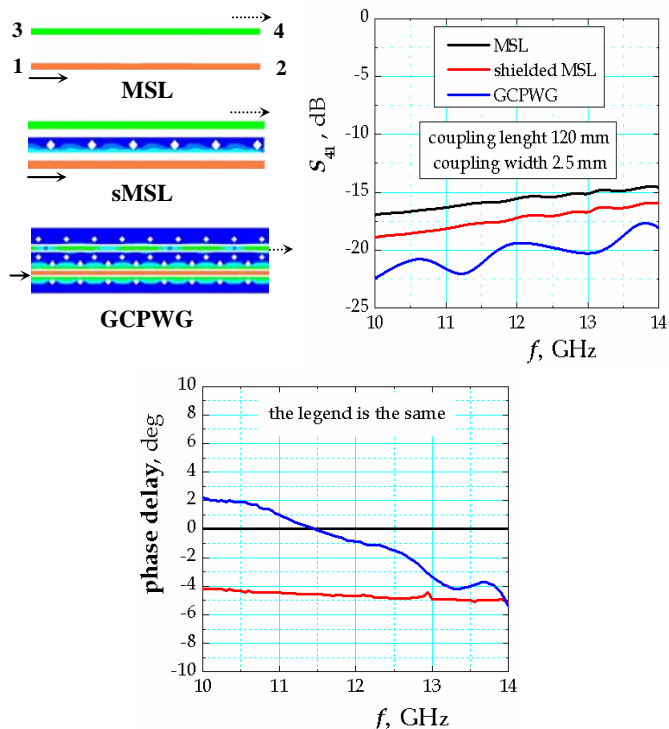
Fig. 19. Crosstalk effects in the transmitted magnitude S_{41} in the coupled line and influence over the phase delay in the main line in three types of coupled 50-Ohms lines: microstrip line (MSL), shielded MSL (sMSL) and grounded coplanar waveguide (GCPWG) (RO3203 substrate; $h = 0.254$ mm; coupled length = 120 mm; distance between the coupled line = 2.5 mm (between the strip axes); distance between the via holes = 3.6 mm)

V. GROUNDING EFFICIENCY

The last problem in our considerations is the grounding efficiency, which in case of multilayer antennas is extremely important [9]. The problem is that the "RF grounding" is considerable more difficult than the low-frequency grounding and usually need a dense array of grounding via holes. One illustrative example for the coupling between two LNA's is given in Fig. 20. The both LNA's are switched on (dc), but only the first is fed by RF signal. The gain of each LNA is ~25 dB. At 8-mm distance between the devices, the ineffective grounded back of the PCB plate of the 1st LNA excites the second LNA by a parasitic RF signal at –15 dB level (this is outside the operational frequency bandwidth 10.2-11.75 GHz). This effect (confirmed by NFS) is fully enough to destroy the operation of the 2nd LNA. The parasitic signal can be absorbed up to –27 dB, if 1-mm thick rubber absorber sheet has been used on the PCB back of the 1st LNA.
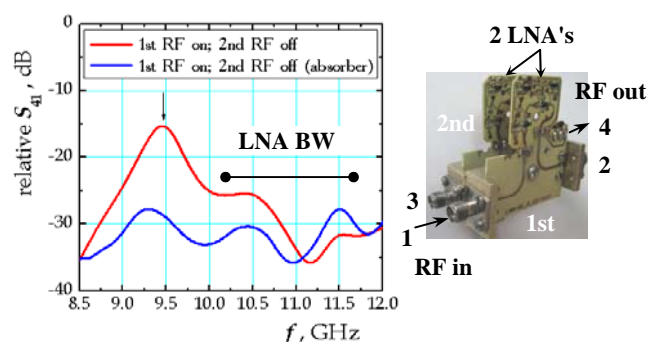
Fig. 20. Measured signal penetration between a pair of 2-stage LNA's (face-to-back coupling at distance 8 mm). The RF signal is passed through port 1 of the 1st LNA; the output is the port 4 of the 2nd LNA. The parameter S_{41} is determined relatively to the measured parameter S_{43} of the 2nd LNA. Ports 2 and 3 have been terminated by 50-Ohms loads.

VI. CONCLUSIONS

The main contribution of the paper is the reveal of the potential of the near-field measurement method for detection of spurious radiations from passive devices in the microwave frequency range. This method could be used for measurement of active devices in the antenna feeds as well, but this is an aim for future investigations.

VII. ACKNOWLEDGEMENT

REFERENCES

[1] "Handbook of Microstrip Antennas", edited by J. R. James & P. S. Hall, 1998, vol. 2, Ch. 14, pp. 843-850

[2] J. Bozmarov, V. Peshlov, R. Traijkov and P. Dankov, "Application of Microwave Absorbers in Multilayer Antenna

Arrays", 14*th* *Int. Conf. on Microwave, Radar and Wireless Communications MIKON'2002, Gdansk, Poland*, May 2002, pp. 221-224

[3] V. Peshlov, I. Slavkov and P. Dankov, "Optimized Meandered Microstrip Feeds for Planar Antenna Arrays", *Proc. EuMC-2001, vol 3,* Excel, London, UK, Sept. 2001, pp. 257-260

[4] B. J. Rubin, B. Singh, "Study of Meander Line Delay in Circuits Boards", IEEE Trans. Microwave Theory Tech., MTT-48, No.9, Sept. 2000, pp. 1452-1460

[5] Zeland Software Inc., IE3D User's Manual;

[6] "Electromagnetic Compatibility of Integrated Circuits", ed. S.B. Dhia, M. Ramdani and E. Sicard, Springer Science + Business Media, Inc., 2006, ch. 4

[7] S. Yuferev and E. Saunamaki, "Practical Techniques for Measurements and Computations of Near-Field Absolute Values", EMC Magazine, 2009, pp. 54-61

[8] ANSYS, HFSS User's Manual

[9] S. Kamenopolsky, R. Arnaudov, I. Vineshki, B. Avdjiiski, S. Alexandrov and P. Dankov, "Inexpensive Chip Carriers for 10-Port Phase Controlling MMIC's in the Ku-Band", *59*th *ARFTG Conference*, Seattle, June 2002, pp. 59-68